Critical Temperature Transitions in Laser Mediated Cartilage Reshaping

Brian J.F. Wong[1,2], Thomas E. Milner[3], Hong K. Kim[1], Sergey Telenkov[1], Clifford Chew[1,2] Timothy Kuo[1,2], Derek J. Smithies[1,4], Emil N. Sobol[5], and J. Stuart Nelson[1]

[1]Beckman Laser Institute and Medical Clinic, University of California Irvine, 1002 Health Sciences Road East ,Irvine, CA 92612; [2]Department of Otolaryngology-Head and Neck Surgery, University of California, Irvine, 101 The City Drive, Orange, CA 92868; [3]Biomedical Engineering Program, The University of Texas at Austin, Austin, TX 78712-1084; [4]Triton Commercial Systems Ltd., Christchurch, New Zealand; [5]Department Of Advanced Laser Technologies, Center for Technological Lasers, Russian Academy of Sciences, 2, Pionerskaya, Troitsk, Moscow Region 142092

ABSTRACT

In this study, we attempted to determine the critical temperature [$\mathbf{T_c}$] at which accelerated stress relaxation occurred during laser mediated cartilage reshaping. During laser irradiation, mechanically deformed cartilage tissue undergoes a temperature dependent phase transformation which results in accelerated stress relaxation. When a critical temperature is attained, cartilage becomes malleable and may be molded into complex new shapes that harden as the tissue cools. Clinically, reshaped cartilage tissue can be used to recreate the underlying cartilaginous framework of structures such as the ear, larynx, trachea, and nose. The principal advantages of using laser radiation for the generation of thermal energy in tissue are precise control of both the space-time temperature distribution and time-dependent thermal denaturation kinetics. Optimization of the reshaping process requires identification of the temperature dependence of this phase transformation and its relationship to observed changes in cartilage optical, mechanical, and thermodynamic properties. Light scattering, infrared radiometry, and modulated differential scanning calorimetry (MDSC) were used to measure temperature dependent changes in the biophysical properties of cartilage tissue during fast (laser mediated) and slow (conventional calorimetric) heating. Our studies using MDSC and laser probe techniques have identified changes in cartilage thermodynamic and optical properties suggestive of a phase transformation occurring near 60^{o}C.

Keywords: cartilage, cosmetic surgery, plastic surgery, otolaryngology, orthopedic surgery, Nd:YAG laser, cartilage reshaping, infrared radiometry, light scattering, stress relaxation

1.0 INTRODUCTION

1.1 Cartilage Biology

Cartilage is a complex macromolecular tissue composed of 80% water, 13% collagen (Type II), and 7% protein-polysaccharide (proteoglycans). The collagen and proteoglycan molecules are synthesized by the chondrocyte, the constitutive cell of cartilage tissue (1). The extracellular matrix of cartilage is a fiber-reinforced gel formed by a three-dimensional network of proteoglycan molecules (100 - 200 MD) which possess negatively charged ion groups (SO_3^{--} and COO^{-} moieties) (2) enmeshed in collagen fibers. The resultant electrostatic repulsion between charged groups results in the expansion of the proteoglycan molecules that is limited by the surrounding tensile collagen framework. The negative charge density is only partially balanced by free counter ions (Ca^{++} and Na^{+}) in solution. This electrical imbalance results in an intrinsic tissue turgor termed the Donnan osmotic pressure (3-5), or at a macroscopic level, internal stress. As a consequence, compressive mechanical deformation of the cartilage is resisted by the screened Coulomb potential between the negatively charged moieties residing on adjacent proteoglycan units (6).

Part of the SPIE Conference on Lasers and Optical Technology in Otolaryngology • San Jose, California • January 1998
SPIE Vol. 3245 • 0277-786X/98/$10.00

The extrinsic morphology of cartilage is determined by the interplay of these ionic forces, ion and fluid flow in the matrix, and the tensile properties of the collagen mesh (4,5).

1.2 Clinical Use of Cartilage Grafts in Surgery

Native cartilage tissue undergoes shape change and warping as a result of surgical manipulation. Gillies noted that if a cartilage specimen is carved with sparing of the perichondrial soft tissue on the opposite side, the graft would curve with concavity being on the perichondrial surface (7). He, therefore, recommended that the perichondral soft tissue be removed prior to implantation. Gibson et al. studied a 30 year clinical series of autologous cartilage grafts used in nasal reconstruction and observed warping even in cases where perichondrium was entirely removed. Gibson developed the concept of "balanced cross sections" and formulated the fundamental principles that are still used today to minimize warping in cartilage tissue grafts during reconstructive surgery (8). In 1967, Fry demonstrated the dependence of this phenomenon on both the proteoglycans and collagen in the cartilage and introduced the concept of "interlocked stresses" (9,10). These early studies focused on the prevention of unwanted shape change in cartilage during grafting. In practice, head and neck reconstruction often requires just the opposite effect in that cartilage must be fashioned into curvilinear shapes.

1.2 Limitations of Traditional Cartilage Graft Shaping

Congenital malformation, trauma, and ablative oncologic surgery can result in loss or severe disruption of the underlying structural framework of the upper airway and aesthetic facial features. Conventional reconstructive techniques involve the grafting of autologous cartilage (harvested from the rib, ear or nasal septum) to the damaged areas. In these approaches, the graft is carved, sutured, and/or morselized to recreate the shape of the absent tissue. As a consequence, abundant normal healthy cartilage tissue is discarded. Because only a limited amount of cartilage is available from harvest sites, conventional reconstructive techniques are frequently problematic, and aggressive harvest may lead to significant donor site morbidity. Some cartilaginous malformations in the head and neck may be treated using surgical techniques that do not require free cartilage grafting, but rather focus on altering the shape of pre-existing cartilage in situ using traditional reconstructive techniques. These methods have the same limitations as grafting techniques, also require open (non-endoscopic) surgical approaches and may result in undesirable irreversible tissue changes.

1.3 Laser Mediated Cartilage Reshaping

The reshaping of cartilage via laser-mediated stress-relaxation was introduced by Sobol and colleagues in 1993 using ex-vivo animal and human cartilage (11-17). Initially, it was observed that laser irradiation of cartilage specimens under mechanical deformation resulted in the permanent reshaping of the tissue(11,12) without evidence of carbonization or ablation. In later studies thermocouple temperature measurements combined with tensiometric measurements of internal stress suggested that marked stress relaxation occurred when tissue temperature reached approximately 60-70^{o}C. Light microscopy suggested that limited histologic evidence of chondrocyte injury (18). While the underlying molecular basis for thermal mediated stress relaxation is incompletely understood, the mechanism of action is thought to involve: 1) a temperature dependent bound-to-free water transition in the cartilage matrix; 2) selective collagen or proteoglycan denaturation; 3) local mineralization of proteoglycan subunits with free cations (chiefly Ca^{++}); and 4) reorganization of van der Waals bonds and weak interactions within the proteoglycan macromolecules. Laser irradiation can reshape autologous donor cartilage grafts into mechanically stable shapes and may potentially be used reconstruct complex anatomic structures such as the external ear without significant loss or waste of harvested tissue. The reshaping process is potentially reversible and adaptable for use in minimally invasive and endoscopic procedures. In contrast to traditional reconstructive surgical techniques, no suturing, carving, or morselization is required to relieve or balance the elastic forces within the cartilage.

To date only three in-vivo laser cartilage reshaping studies have been performed and neither of these investigations monitored changes in tissue temperature, optical properties, or internal stress nor was a feedback control system used to modulate laser irradiation. Wang et al. successfully reshaped crushed canine tracheal cartilage via an endoscopic approach using a pulsed Nd:YAG laser (λ= 1.44 μm), but the cartilage

and its overlying mucosa were simultaneously irradiated (19,20). Sobol and colleagues created sharp curves in the external ears of domestic pigs using Ho:YAG laser (λ=2.12 μm) radiation delivered transcutaneously with a fiberoptic cable (21). In Greece, a small series of patients underwent laser mediated nasal septal cartilage reshaping for nasal airway obstruction using a CO_2 laser (λ=10.6 μm) but the results of this study were mixed and difficult to interpret (E. Sobol, personal communication). While these limited animal and human studies have demonstrated clinical feasibility, neither safe energy parameters for laser assisted cartilage reshaping are known, nor has a reliable feedback technique to optimize and monitor treatment been identified.

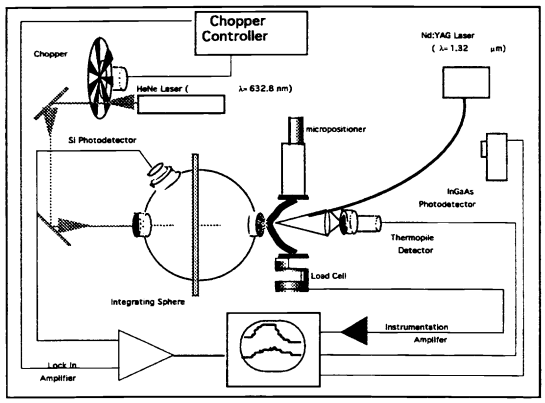

Figure 1: Schematic of instrumentation used for measurement of integrated backscattered light intensity $\mathbf{I(t)}$, internal stress $\sigma(t)$, and radiometric surface temperature $\mathbf{S_c(t)}$. An InGaAs photodetector is used to detect the initial Nd:YAG laser pulse and trigger data acquisition.

1.4. Changes in the Thermal, Optical, and Mechanical Properties of Cartilage During Laser Irradiation

In our preliminary investigations (22,23), simultaneous measurements of radiometric surface temperature [$\mathbf{S_c(t)}$], internal stress [$\sigma(t)$], and integrated backscattered light intensity [$\mathbf{I(t)}$] from a probe HeNe laser (λ=632.5 nm, 5 mW) were recorded from a cartilage specimen during irradiation with a Nd:YAG laser (λ=1.32 μm, 6.94 W, 38.45 W/cm^2). The cartilage specimen was held in compression between an aluminum plate attached to a calibrated single-axis micropositioner and a thin beam load cell coupled to an aluminum mounting plate (**Figure 1**). The internal stress [$\sigma(t)$ **(a.u.)**] across the cartilage specimen was adjusted by translating the micropositioner. Radiometric surface temperature [$\mathbf{S_c(t)}$ (^{o}**C**)] of the laser irradiated cartilage was monitored using a thermopile sensor centered on the Nd:YAG laser spot (on the specimen). Backscattered HeNe laser light incident on the opposing surface of the irradiated cartilage specimen was collected in an integrating sphere and measured using a silicon photodetector and preamplifier to yield integrated back scattered light intensity $\mathbf{I(t)}$. The HeNe beam was incident at the center of the Nd:YAG laser spot on the specimen. HeNe laser light intensity was amplitude modulated (10 kHz) with a mechanical chopper and synchronously detected by a lock-in amplifier. The fractional change in integrated backscattered light intensity $\Delta\mathbf{I(t)/I_0}$ was calculated by measuring the change in $\mathbf{I(t)}$ relative to baseline $\mathbf{I_0}$ recorded prior to the onset of Nd:YAG laser irradiation.

Radiometric surface temperature $\mathbf{S_c(t)}$, internal stress $\sigma(t)$, and integrated backscattered light intensity $\mathbf{I(t)}$ were recorded during laser irradiation of the central region of a cartilage specimen undergoing compressive deformation. Internal stress, $\sigma(t)$ was recorded simultaneously with either $\mathbf{I(t)}$ or $\mathbf{S_c(t)}$, as our current apparatus was not configured to measure three signals simultaneously. Following observation on the lock-in amplifier of the peak value for $\mathbf{I(t)}$ laser irradiation was terminated. Typically, irradiation continued for 2-4 seconds beyond the peak (identification of the peak required observation of a downward trend in $\mathbf{I(t)}$ on the amplifier). Following the onset of laser irradiation, $\mathbf{I(t)}$ underwent a characteristic increase and subsequent decrease with a peak occurring when $\mathbf{S_c(t)}$ reached about 65 ^{o}C.

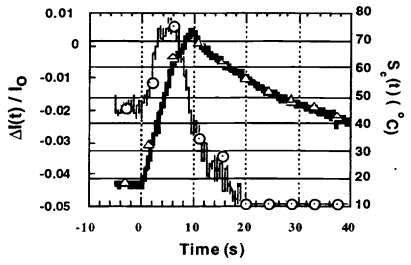

Figure 2: Simultaneous measurements of radiometric surface temperature [$S_c(t)$ (°C)] and fractional change in integrated back scattered light intensity [$\Delta I(t)/I_0$]. Laser irradiation time was 9.5 seconds. $\Delta I(t)/I_0$ initially increased and reached a peak between 4 to 6 seconds of applied laser irradiation. In this time interval, $S_c(t)$ approached 65°C and a slope change in was observed. Despite continued laser irradiation and surface temperature increase, $\Delta I(t)/I_0$ continued to decrease. (-Δ---Δ---Δ--$S_c(t)$, -o---o---o--$\Delta I(t)/I_0$)

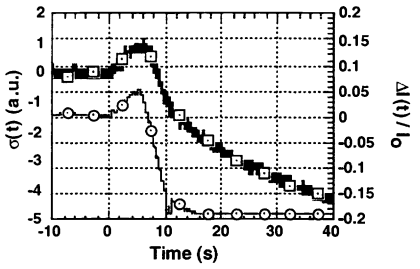

Figure 3: Simultaneous measurements of internal stress $\sigma(t)$ (normalized, arbitrary units) and fractional change in integrated back scattered light intensity $\Delta I(t)/I_0$. Laser irradiation time was 10 seconds. The peaks for $\Delta I(t)/I_0$ and $S_c(t)$ occur simultaneously, despite continued laser irradiation. Prior to the onset of laser radiation (-10 to 0 seconds), the base line stress relaxation rate for native cartilage is recorded.(-|—|—|--$\sigma(t)$, -o—o—o—$\Delta I(t)/I_0$). The decrease in $\sigma(t)$ accelerates following laser irradiation.

Figure 2 depicts cartilage radiometric surface temperature $S_c(t)$ and the fractional change in integrated back scattered light intensity $\Delta I(t)/I_0$ as a function of time during and following laser irradiation. We noted a pronounced change in the slope of $S_c(t)$ at approximately 65°C and six seconds into laser irradiation. During the same time interval, $\Delta I(t)/I_0$ reaches a maximum, attains a plateau, and then decreases monotonically. Laser irradiation was continued over 9.5 seconds and the peak for $\Delta I(t)/I_0$ occurred (4-6 seconds) prior to the cessation of laser radiation. These findings are consistent with our previous observations in porcine auricular cartilage (24).

Figure 3 depicts the simultaneous measurement of fractional change in integrated back scattered light intensity [$\Delta I(t)/I_0$] and internal stress $\sigma(t)$ during and after 10 seconds of laser irradiation. The stress relaxation rate of native (non-irradiated) porcine septal cartilage held in compression between a load cell and micropositioner is illustrated from -10 to 0 seconds.

Mechanical relaxation in the absence of laser irradiation takes a prohibitively long period of time which is impractical in the operating room. Laser irradiation accelerates this process via a thermally mediated mechanism. At the onset of laser irradiation (0-4 seconds), internal stress $\sigma(t)$ actually increases and approaches a plateau that is coincident with the observed plateau for $I(t)$ (and also occurs when $S_c(t)$ is approximately 65°C). During the plateau period (4-8 seconds), both $d\sigma(t)/dt$ and $d(\Delta I(t)/I_0)/dt$ approach zero, and then subsequently decrease. Interestingly, $d\sigma(t)/dt$ continues to decrease at an accelerated rate well after irradiation has ceased. Although the origin of the transient increase in $d\sigma(t)/dt$ during laser irradiation is not clear (0-4 seconds), the process may represent water expansion in the irradiated tissue volume during laser heating.

Collectively, the observed trends in $\sigma(t)$, $I(t)$, and $S_c(t)$ suggest the cartilage is undergoing a phase transformation (14). Inasmuch as the maxima of both light scattering and internal stress are nearly coincident, $\Delta I(t)/I_0$ may be used as a control signal to optimize the process of laser-assisted re-shaping. Light scattering experiments provide insight into several possible mechanisms. When surface temperature reaches about 65° C, a stationary region in the fractional change in integrated back scattered light intensity signal ($d\Delta I(t)/I_0/dt = 0$) is observed . Sobol et al. have suggested that the change in light scattering properties of cartilage may be due to the formation of isolated regions of water movement with anomalous refractive index values leading to an increase in back scattered light intensity (13). As the tissue is heated, additional regions of the

tissue undergo this change in refractive index and eventually coalesce resulting in a decrease in the overall scattered light signal. At the molecular level, Sobol et al. have suggested that water in the cartilage is undergoing transition from a bound state (to proteoglycans or collagen) to a free or mobile state. This bound-to free transition is temperature dependent. Hence during laser heating, water moves through the matrix, and charged moieties on the proteoglycans are no longer shielded by water molecules. In a cartilage specimen under mechanical stress, cooling results in the re-formation of weak bonds (hydrogen, polar bonds) between proteoglycan groups and water, and new stable shapes are formed. Alternatively, the process of stress relaxation may involve partial denaturation of collagen. A slope change in $\mathbf{S_C(t)}$ occurs at about 65°C that is synchronous with changes in $\mathbf{I(t)}$ where $\mathbf{d\Delta I(t)/I_0/dt}$= 0, and this change in the heating rate at the surface suggest a change in cartilage thermal properties. 65°C is the approximate denaturation temperature and suggested that the collagen helices may unwind upon heating and then recoil as the tissue is allowed to cool (25).

2.0 MATERIALS AND METHODS

2.1. Rose Chamber Light Scattering Measurements

Using single element infrared detectors, a critical temperature [$\mathbf{T_c}$] of about 65°C was observed, and accompanied characteristic changes in integrated backscattered light intensity [$\mathbf{I(t)}$] and internal stress [$\sigma\mathbf{(t)}$](23-25). While radiometric measurements of temperature are non-contact and relatively fast, they are limited in that the infrared emissions from only the most superficial layers of the tissue are detected. The temperature distribution within the cartilage tissue during laser irradiation is not uniform and, due to evaporative cooling the temperature at the surface, is lower than deeper tissue layers in the cartilage. Further, measurements of $\mathbf{I(t)}$ and $\sigma\mathbf{(t)}$ reflect changes in the entire region of the specimen undergoing heating by the Nd:YAG laser, and not just the most superficial layer of tissue.

In order to minimize the effect of evaporative cooling and the non-uniform temperature distribution within the cartilage tissue created by laser mediated heating, $\mathbf{I(t)}$ was recorded from cartilage tissue immersed in saline solution and subjected to a slow heating rate. A square porcine nasal septal cartilage specimen was inserted into a saline filled Rose chamber (**Figure 4**). A Rose chamber is a sealed, sterile chamber (containing tissue

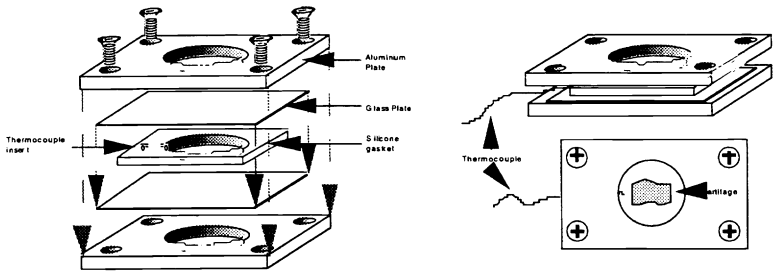

Figure 4: Rose chamber schematic. A Rose chamber is a sealed, sterile chamber (containing tissue specimens and saline) created by "sandwiching" an impermeable silicone rubber gasket between two large silica microscope slides held in place with aluminum plates fastened at the corners with screws. Gaskets of varying thickness can be adjusted so that the cartilage front and back surfaces do not come in direct contact with the slide glass. The tip of a thermocouple was inserted through the silicone gasket into the chamber in close approximation to the cartilage.

specimens and saline) created by "sandwiching" an impermeable silicone rubber gasket between two large silica microscope slides held in place with aluminum plates fastened at the corners with screws. Gaskets of varying thickness can be adjusted so that the front and back surfaces of the cartilage do not come in direct contact with the glass slide. The tip of a Teflon insulated Type E thermocouple (Chromega-Constantan, 0.005" wire diameter, 5TC-TT-E-36-36 with cold junction compensator, M60/1290, MCJ Series, Omega Co., Stamford, CT) was inserted through the silicone gasket into the chamber in close approximation to the

cartilage. The voltage at the cold junction compensator was amplified and low band pass filtered (Stanford Research Systems, SRS 650, Sunnyvale, CA) and displayed on a digital storage oscilloscope.

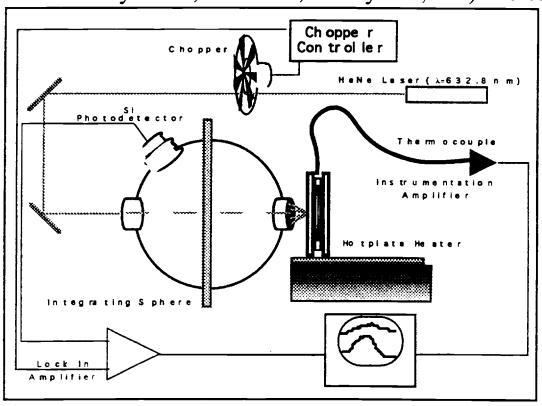

Figure 5: Schematic of instrumentation used for measurement of integrated back scattered light intensity **I(t)** and chamber temperature of a Rose chamber heated with a laboratory hotplate. The cartilage specimen is completely immersed in saline within the chamber, and a HeNe laser beam is focused on the central part of the specimen (intensity modulated- 10 kHz). A silicon photodetector and lock-in amplifier measured the integrated back-scattered light signal ***I(t)***. A thermocouple is used to measure the chamber temperature.

Calibration was performed using a mercury thermometer and a water bath heated from 20 to 100 °C. The response of the thermocouple was linear over the range studied. The assembled Rose chamber with enclosed cartilage tissue was placed on a laboratory hot plate heater (**Figure 5**) and back-scattered light was measured using an experimental set-up similar to that described in **Figure 1** while the chamber was slowly heated to a pre-set endpoint temperature. A non-uniform temperature distribution or thermal gradient within the chamber is unlikely given the slow rate of temperature change, and high thermal conductivity of the aluminum mounting plates.

2.2. Modulated Differential Scanning Calorimetry

Differential scanning calorimetry (**DSC**) is a traditional thermal analysis technique which is used to measure temperatures and heat flows associated with transitions in materials as a function of time and temperature. Modulated differential scanning calorimetry (**MDSC**) differs in that a sinusoidal heating curve is superimposed on the conventional linear heating curve of DSC. Deconvolution of the resultant profile during cyclic heating allows determination of the total heat flow (as obtained in conventional DSC) and its reversible (heat capacity related) and kinetic (non-reversible) components. Disc shaped cartilage specimens were made using a 5 mm diameter tissue punch and sliced to approximately 0.5 mm in thickness (mass 15.3 mg). The specimen was encased within a small metal pan and placed in the calorimeter (MDSC 2920 Differential Scanning Calorimeter, TA Instruments, New Castle, DE). The specimen and calorimeter were brought into thermal equilibrium at 25°C, and the calorimeter temperature was increased at a baseline rate of 5.5 °C/minute superimposed with a sinusoidal heating profile (60 second period, amplitude of 0.7965°C). Total (mW) reversible and non-reversible heat flows were calculated as a function of temperature.

2.3. Time Dependence of Reshaping

In order to accomplish effective laser mediated reshaping: 1) the temperature in the irradiated cartilage tissue must exceed a critical temperature [$\mathbf{T_c}$] for accelerated stress relaxation to occur; and 2) the cartilage must remain at this temperature for a minimum time interval [$\tau_{\mathbf{min}}$]. In the preliminary studies(22,23), radiometric temperature measurements, light scattering, and calorimetry gave estimates for $\mathbf{T_c}$ to be in the temperature range of 55-65°C which is the minimum temperature at which stress relaxation occurs. It should be noted that, apart from the radiometric surface temperature measurement (1.4), neither Rose chamber light scattering measurements (2.1) nor MDSC (2.2) incorporated simultaneous measurements of tissue internal stress [$\sigma(t)$]. As the true value for $\mathbf{T_c}$ is unknown, we chose 70°C as the temperature to perform the following series of studies.

Nasal septal cartilage specimens (free of perichondrium) were cut into strips measuring approximately 12 x 35 x 2.7 mm. These specimens were wrapped around a plastic dowel (8 mm diameter), secured in place with thin stainless steel sewing needles, and immediately placed in a heated saline bath maintained at a constant temperature of 70° C for varying time intervals (120, 60, 30, 15, 10, and 9 seconds). The immersion was used to heat cartilage because: 1) thin cartilage specimens reach thermal

equilibrium rapidly; and 2) the duration of heating can be easily controlled, allowing a simple estimation of τ_{min} at a given temperature. Immediately following immersion, the secured cartilage specimens were placed in a second bath at an ambient temperature and allowed to equilibrate for 15 minutes. The need for this equilibration/rehydration step has been previously described (23). Following this second immersion, the retaining pins were removed. Cartilage specimens were stored in saline at 5°C and serially photographed.

2.4. Infrared Focal Plane Array (IR-FPA) Measurements of Cartilage Surface Temperature During Laser Mediated Reshaping.

A limitation of single element infrared detectors and thermopiles is that the radiometric signal is an average from a specific location on the specimen surface. For the present studies, under optimal conditions, this specific location should be very small Cartilage specimens were irradiated with a Nd:YAG laser (λ= 1.32 μm, 50 Hz PRR NewStar Lasers, Auburn, CA) with variable exposure times. Light was delivered by a 600 μm core-diameter silica multimode optical fiber and at the center of the laser spot. Size was limited by the infrared optics of the system, and the present thermopile system (1.4) imaged temperature over a 3mm diameter spot. In order to determine precisely the spatial distribution of temperature, an IR-FPA (Galileo, Amber Engineering, Goleta, CA) was used to measure surface temperature distribution (26). A cartilage specimen measuring 23 x 10 x 2 mm was held in compression with a micropositioner as illustrated in **Figure 6** and was irradiated with a Nd:YAG laser for 9 seconds (4 W, 5 mm diameter while **I(t)**, σ(t), and the spatial distribution of temperature $\mathbf{S_c(t,x,y)}$ (256 x 256, 30 μm/pixel) were simultaneously recorded. Using pre-recorded calibration data and software visualization utilities (AVS, Waltham MA) running on a Digital Equipment Workstation platform (Digital Equipment Corporation, Maynard, MA), average radiometric temperature $\mathbf{[S_{avg}(t,d)]}$ was determined within a fixed circular region centered on a variable diameter (**d**) laser spots (i.e., d= 0.4, 1.6, 3.2, 4.8, or 6.4 mm).

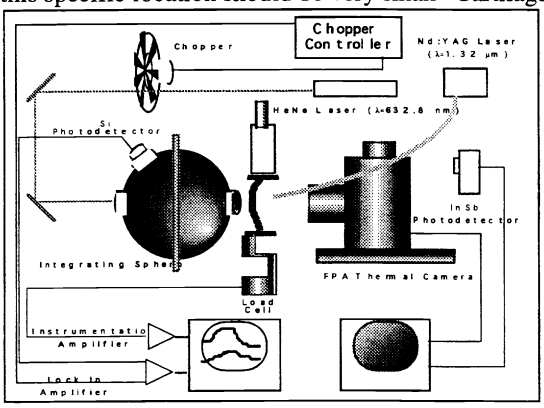

Figure 6: Schematic of instrumentation used for measurement of integrated back scattered light intensity **I(t)**, internal stress σ(t), and radiometric surface temperature $\mathbf{S_c(x,y,t)}$. The set-up is similar to that illustrated in **Figure 1**. The infrared focal plane array collects data from an 8 x 8 mm square region of interest. Individual pixel resolution is 30μm.

3.0 RESULTS

3.1. Rose Chamber Light Scattering Measurements

I(t) was observed to increase and subsequently decrease with a peak occurring when chamber temperature reached approximately 55°C [chamber endpoint temperature was set at 70°C **(Figure 7)**]. Repeating this experiment, with the same cartilage specimen following storage in saline for 24 hours at 5°C, demonstrated only an increase and plateau in **I(t)** **(Figure 8)**. Using a fresh cartilage specimen and a chamber endpoint temperature of only 50°C, **I(t)** was observed to increase and plateau despite prolonged heating **(Figure 9)**.

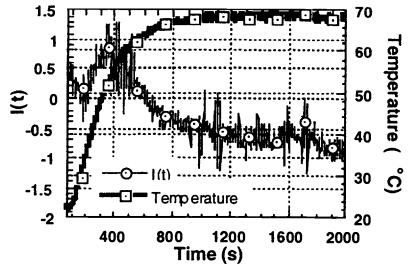

Figure 7: Measurement of integrated backscattered light intensity [**I(t)**] as a function of temperature within a Rose chamber. **I(t)** peaks when chamber temperature reaches approximately 55°C.

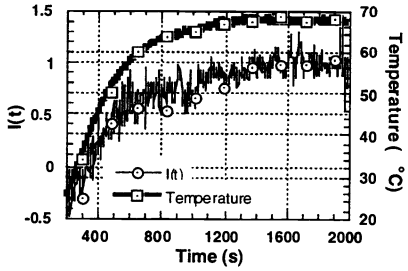

Figure 8: Effect of reheating cartilage in a Rose chamber. The cartilage specimen that heated in **Figure 7** was allowed to rehydrate in saline solution for 24 hours at 5°C and then reheated in the Rose chamber to an endpoint temperature of 70°C. In contrast to native tissue, **I(t)** does not peak but reaches a plateau.

3.2. Modulated Differential Scanning Calorimetry

Figure 10 shows total heat flow, reversible heat flow, and non-reversible heat flow as a function of temperature. Reversible heat flow reflects energy flow into non- volatile specimen components, while non-reversible heat flow represents energy deposited into volatile components such as water. Note the difference in the scales for the two Y-axis; the reversible heat flow is a relatively small component of total heat flow and is not measurable using conventional DSC. In this cartilage specimen, reversible heat flow

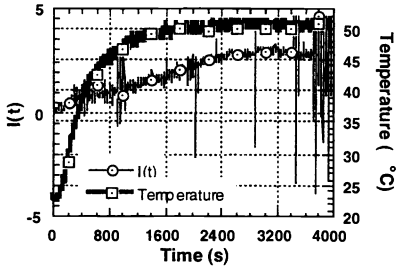

Figure 9: Rose chamber endpoint temperature set to 50°C. **I(t)** does not peak when chamber temperature does not exceed a critical value (approximately 55°C, not illustrated). When endpoint temperatures are below the threshold, no peak in **I(t)** is observed and a plateau is reached despite prolonged heating.

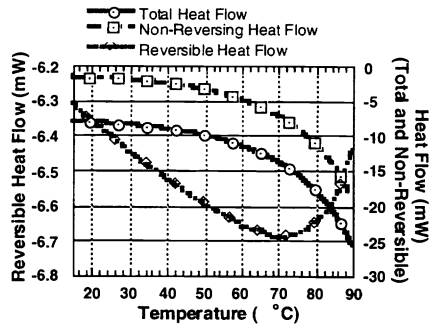

Figure 10: MDSC measurements of cartilage. A 15.3 mg cartilage specimen was placed in the calorimeter. Reversible, non-reversible, and total heat flow measurements were obtained as a function of temperature. Note that reversible heat flow (heat flow into the cartilage specimen) reaches a peak at approximately 70°C.

into the specimen increased until a temperature of approximately 65°C is attained and then decreases. Reversible heat flow is proportional to the heat capacity c_p for the non-volatile components of the specimen. Hence these MDSC measurements suggest that the thermal properties of cartilage change at 65° C. There are limitations to the accuracy of the present MDSC measurements in that temperature may differ slightly from cartilage temperature due to heat conduction factors related to specimen size.

3.3. Time Dependence of Cartilage Reshaping

Cartilage reshaping occurred in all specimens heated for greater than one minute in the 70°C saline bath; specimens which remained in the heated saline bath for less than this time underwent minimal shape

change. Straight pieces of cartilage subsequently became curved. The radius of curvature of the reshaped specimens was much larger than the radius of the shaping dowel (8 mm). This result is consistent with the fact that reshaping (stress relaxation) occurs only in regions of the tissue that are under mechanical stress. When a straight cartilage specimen is wrapped around a dowel, the region of "maximum stress" (13) is at the base of this "U" shaped bend. Under these conditions (water bath immersion, constant temperature), τ_{min} is estimated to be at least one minute although this method of heating differs markedly from laser mediated techniques. While it is possible to reshape cartilage using this simple method, the slow rates of heating employed here may result in stress relaxation involving denaturation processes and subsequent cell death. The time-dependent temperature profile in laser irradiated cartilage is characterized by rapid temperature elevations accompanied by rapid thermal relaxation; time-dependent denaturation processes are minimized.

3.4. IR-FPA Measurements of Cartilage Surface Temperature During Laser Mediated Reshaping

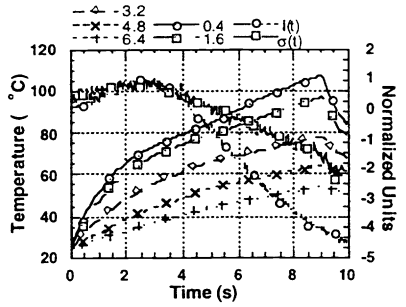

Figure 11: Simultaneous measurement of **I(t)**, **σ(t)**, **S_{avg}(t,d)** for **d= 0.4, 1.6, 3.2, 4.8, 6.4.** An IR-FPA was used to acquire surface temperature measurement as a function of location and time. **S_{avg}(t,d)** was calculated using software visualization utilities.

In **Figure 11,** simultaneous recordings of integrated back scattered light intensity **[I(t)]**, internal stress **[σ(t)]**, and average surface temperature **[S_{avg}(t,d)]** are illustrated during 9 seconds of laser irradiation. As the diameter **[d]** of the region of interest is increased, peak temperature decreases, as expected. In section 1.4, a slope change in **S_c(t)** was observed when both **I(t)** and **σ(t)** peaked. In **Figure 11**, this change in slope is only observed when **d** is less than about 3 mm. As previously noted (1.4), characteristic changes in **I(t)** and **σ(t)** are observed following approximately 3 seconds of irradiation. The cartilage specimen was irradiated for 9 seconds in order to demonstrate two points: 1) peaks in **I(t)** and **σ(t)** occurred even in the presence of sustained irradiation; and 2) radiometric surface temperature measurements were sensitive over the area in which the temperature was being averaged. In our previous studies, **S_c(t)** was recorded using single element detector systems (22-24). These systems (detector and focusing IR optics) determine average temperature over a region of interest which is defined by the point spread function and varied from 1 to 3 mm; this area may not match the size of the region of tissue undergoing stress relaxation during laser irradiation. We used an IR-FPA to determine the precise spatial distribution of temperature in cartilage during laser irradiation, and this information allowed meaningful interpretation of temperature measurements from single element devices.

4.0 DISCUSSION AND CONCLUSIONS

Cartilage undergoes temperature dependent stress relaxation accompanied by changes in its optical, mechanical, and thermal properties. While lasers have been used to heat cartilage and reshape native tissue, a complete understanding of the molecular basis for these observed biophysical changes is unknown. The principal objective of this study was to determine the critical temperature for accelerated stress relaxation in cartilage tissue and thus provide a basis with which laser mediated cartilage reshaping may be optimized. The process of reshaping is temperature dependent and earlier studies have shown a transition temperature zone at approximately 65°C.

4.1 Rose Chamber Investigations

Laser irradiation of cartilage specimens results in non-uniform heating of the tissue, as energy deposition (and heating) is directly related to the irradiance which varies with tissue depth. Light

distribution cartilage has not been modeled as the absorption and scattering coefficients in cartilage at the wavelengths used in this study are unknown. The non-uniform nature of laser mediated heating results in asynchronous stress relaxation in different regions of the tissue. Integrated backscattered light intensity **[I(t)]** is a measure of diffusely scattered light from the laser. Because the HeNe is highly scattered in cartilage (in comparison to the Nd:YAG laser), changes in **I(t)** are due to backscattering interactions in the superficial tissue layers on the back surface of the specimen (**Figure 1**). Optimally, **I(t)** should be measured during uniform heating of the cartilage specimen.

In laser mediated cartilage reshaping, thick (1.5-4 mm) tissue specimens are heated to at least 65°C. It is not possible to heat such thick specimens uniformly using laser irradiation. Uniform heating could be accomplished using non-laser sources (ultrasonic, conventional oven, microwave) but the relatively slow heating times of these devices would result in marked tissue desiccation. In order to examine precise temperature dependent changes in light scattering as a function of temperature, we heated cartilage in saline within a Rose chamber. While these conditions differ markedly from laser mediated heating in terms of time course, these studies allowed the creation of uniform temperature profiles within the cartilage without specimen dehydration.

Figure 7 demonstrates that at approximately 55°C, **I(t)** reaches a peak and subsequently decreases. When this specimen is stored in saline for 24 hours at 5°C and the experiment is then repeated, this peak in **I(t)** disappears. These findings are strikingly similar to previous observations (22,23). While this experimental arrangement differs from our previous configurations (performed in air, laser heated, and under mechanical stress vs. water heating at a slow rate without mechanical stress), these findings do suggest: (1) a critical transition temperature $\mathbf{T_c}$ exists near 55°C under conditions of slow heating, and (2) the changes in the optical properties in cartilage tissue are irreversible following prolonged exposure to this temperature range under slow heating conditions. Notably, when the Rose chamber endpoint temperature is set to only 50°C, **I(t)** was only observed to increase and plateau despite prolonged heating (**Figure 9**).

4.2 MDSC

Modulated scanning differential calorimetry (MDSC) was used to evaluate temperature dependent changes in cartilage primarily because of its: 1) ability to analyze properly complex transitions (i.e., enthalpic relaxations, crystallization events, glass transitions), 2) high sensitivity, and 3) high resolution in contrast to conventional differential scanning calorimetry. **Figure 10** illustrates total, non-reversible and reversible heat flows as a function of temperature. At about 70°C, reversible heat flow (heat flow into the specimen) reaches a maximum and subsequently decreases. These MDSC studies were performed under conditions in which the volatile components of cartilage evaporated (non-reversible heat flow), and hence reversible heat flow measurements only reflect changes in the matrix components of cartilage. While these calorimetric studies are similar to the Rose chamber studies in that tissue was slowly heated, it differs in that water was allowed to evaporate (measurements were performed at constant volume). The presence of a peak in reversible heat flow at about 70°C is in agreement with temperature dependent changes in the optical and mechanical properties we have observed as noted above. These results are preliminary, and further studies are planned to obtain more precise measurements while performing optical measurements of cartilage during MDSC experiments.

4.3. Time Dependence of Reshaping

Heated water bath immersion is potentially a extremely useful method for reshaping cartilage. The principal advantages are: 1) no dehydration, 2) low cost, 3) simple, and 4) performed without advanced instrumentation. A uniform temperature distribution in the cartilage tissue rapidly established because the specimen is totally immersed in heated saline. While these are extremely attractive features, the principal disadvantage is that immersion in a 70°C saline bath for approximately one minute likely results in overt chondrocyte injury and probable devitalization of the cartilage tissue. Short immersion times (10, 20, 30 seconds) did not result in a stable shape change. We are presently peforming radio-isotope studies to determine the conditions under which cartilage viability is maintained in response to thermal injury.

4.4 IR-FPA measurements

Initial attempts to determine the critical transition temperature [T_c] during which accelerated stress relaxation begins relied on a small thermocouple inserted into a cartilage specimen (14). While thermocouples do provide precise information, they cannot measure temperature over the region of tissue under direct laser irradiation so that only changes adjacent to the area of exposuret can be estimated. A further limitation of thermocouples was that the probes must be inserted into the specimen, and that is technically difficult to accomplish with precision during surgery and potentially weakens cartilage graft tissue.

In our initial studies, we used single element infrared detectors or thermopiles to estimate radiometric surface temperature from cartilage during laser irradiation (22,24). Radiometry provides a non-contact method of estimating surface temperature which is desirable for clinical applications. Nevertheless, there are limitations to IR radiometry: 1) single element devices have limited spatial resolution determined by the point spread function of the detector and its infrared optics; 2) only the IR emissions from the most superficial tissue layers (10-20 μm) are measured; and 3) evaporative cooling at the surface results in higher temperatures in the deeper layers of the specimen. The focused detector probe area of the liquid N_2 cooled HgCdTe detector used in our initial study measured the average IR emissions from a 1 mm diameter region of interest (24). In later studies, the infrared optics of the thermopile measurements imaged a 2 mm diameter (FWHM) region of interest onto the sensor element (23). In studies using both systems, a noticeable change in the slope of $S_c(t)$ was observed near 65°C. There are two possible explanations for this phenomenon: 1) the thermal properties (conductivity and diffusivity) change at this temperature (which would be consistent with a phase transformation) or 2) axial and radial heat conduction occur.

We used a high resolution IR-FPA to record the spatial distribution of surface temperature during laser irradiation, and determine the average temperature [$S_{avg}(t,d)$] within circular regions of interest (diameter [**d**]). Our main observation is that size of the region of interest over which temperature is averaged, must be significantly smaller than the size of the laser spot. For example, if $S_{avg}(t,d=6.4\ mm)$ is calculated, it will significantly underestimate peak temperatures in the center of the laser spot (**Figure 11**). This is of relevance for the design of clinical devices using low-cost thermopile detectors for temperature feedback control; these devices may *under estimate* surface temperature. The IR-FPA measurements confirm the observation of a slope change in $S_c(t)$ when temperature is averaged over small regions of interest (i.e. 0.4 mm). When large values for **d** are used, a nearly linear temperature rise is observed. Without an analytic model for heat conduction in cartilage, it is not possible to determine what is the contribution of thermal diffusion to the observed changes in $S_c(t)$ versus intrinsic changes in tissue thermodynamic properties. At present, we are developing analytic models to further examine this problem.

5.0 ACKNOWLEDGMENTS

This work was supported by the Office of Naval Research, Department of Energy, Whitaker Foundation, New Star Lasers, Inc., and the National Institute of Health. The authors express their appreciation to Mr. Marvin Gryzys of TA Instruments.

6.0 REFERENCES

1. Muir H. The chondrocyte, architect of cartilage: Biomechanics, structure, function and molecular biology of cartilage matrix macromolecules. BioEssays 1996;17:1039-1048.
2. Roughley P, Lee E. Cartilage proteoglycans; Structure and potential functions. Microscopy Research and Technique 1994;28:385-397.
3. Donnan FG. The Theory of Membrane Equilibria. Chemical Reviews 1924;1:73-90.
4. Lai W, Hou J, Mow V. A triphasic theory for the swelling of hydrated charged soft biological tissues. In: Mow V, Ratcliffe A, Woo S-Y, eds. Biomechanics of diarthroidal joints. New York: Springer-Verlag, 1990:283-312.
5. Lai W, Hou J, Mow V. A Triphasic Theory for the Swelling and Deformation Behaviors of Articular Cartilage. Journal of Biomechanical Engineering 1991;113:245-258.

6. Buschmann MD, Grodzinsky AJ. A molecular model of proteoglycan-associated electrostatic forces in cartilage mechanics. Journal of Biomechanical Engineering 1995;117:180-192.
7. Gillies H. Plastic Surgery of the Face. London: Oxford University Press, 1920.
8. Gibson T, Davis W. The distortion of autogenous cartilage grafts: its cause and prevention. British Journal of Plastic Surgery 1958;10:257-74.
9. Fry H. Interlocked stresses in human nasal septal cartilage. British Journal of Plastic Surgery 1966;19:276-278.
10. Fry H. Cartilage and cartilage grafts: the basic properties of the tissue and the components responsible for them. Plastic and Reconstructive Surgery 1967;40:426-439.
11. Helidonis E, Sobol E, Kavvalos G, et al. Laser Shaping of Composite Cartilage Grafts. American Journal of Otolaryngology 1993;14:410-412.
12. Helidonis ES, Sobol E, Velegrakis G, Bizakis J. Shaping of Nasal Septal Cartilage with the Carbon Dioxide Laser- a Preliminary Report of an Experimental Study. Lasers in Medical Science 1994;9:51-54.
13. Sobol E, Bagratashvili VV, Omel'chenko A, et al. Laser Shaping of Cartilage. Proceedings SPIE 1994;2128:43-49.
14. Sobol E. Phase transformations and ablation in laser-treated solids. New York: John Wiley, 1995.
15. Sobol E, Bagratashvili VV, Sviridov A, et al. Cartilage Reshaping with Holmium Laser. Proceedings SPIE 1996;2623:556-559.
16. Sobol E, Bagratashvili VV, Sviridov A, et al. Phenomenon of Cartilage Shaping using Moderate Heating and its Application in Otorhinolaryngology. Proceedings SPIE 1996;2623:560-564.
17. Sobol E, Sviridov A, Bagratashvili VV, et al. Stress Relaxation and Cartilage Shaping under Laser Radiation. Proceedings SPIE 1996;2681:358-363.
18. Helidonis E, Volitakis M, Naumidi I, Velegrakis G, Bizakis J, Christodoulou P. The histology of laser thermo-chondro-plasty. American Journal of Otolaryngology 1994;15:423-428.
19. Wang Z, Pankratov MM, Perrault DF, Shapshay SM. Endoscopic Laser-Assisted Reshaping of Collapsed Tracheal Cartilage: A Laboratory study. Annals of Otology, Rhinology, and Laryngology 1996;105:176-181.
20. Wang Z, Pankratov MM, Perrault DF, Shapshay SM. Laser-Assisted Cartilage Reshaping: In vitro and in Vivo Animal Studies. Proceedings SPIE 1995;2395:296-302.
21. Sviridov A, Sobol E, Bagratashvili V, et al. In Vivo Reshaping of Pig Ear Cartilage Under a Holmium Laser Radiation. Proceedings SPIE 1998;in press.
22. Wong BJF, Milner TE, Anvari B, et al. Measurement of Radiometric Surface Temperature and Integrated Back-Scattered Light Intensity During Feedback Controlled Laser-Assisted Cartilage Reshaping. Lasers in Medical Science 1997;in Press.
23. Wong BJF, Milner TE, Kim HK, Nelson JS, Sobol EN. Stress Relaxation of Porcine Septal Cartilage During Nd:YAG (λ = 1.32 μm) Laser Irradiation: Mechanical, Optical, and Thermal Responses. Journal of Biomedical Optics 1998;Submitted for publication.
24. Wong BJF, Milner TE, Anvari B, et al. Thermo-Optical Response Of Cartilage During Feedback Controlled Laser-Assisted Reshaping. SPIE Proceedings 1997;2970:380-391.
25. Allain JC, Le Lous M, Cohen-Solal L, Bazin S, Maroteaux P. Isometric Tensions Developed During the Hydrothermal Swelling of Rat Skin. Connective Tissue Research 1980;7:127-133.
26. Milner T, Goodman D, Tanenbaum B, Anvari B, Svaasand L, Nelson JS. Imaging laser heated subsurface chromophores in biological materials: determination of lateral physical dimensions. Physics in Medicine and Biology 1996;41:31-44.